
Gamma-Ray Bursts
A Tribute to Giorgio Palumbo

Brian McBreen



~1978

1969



Radio signals from air showers at 22 MHz¹

J. R. PRESCOTT AND G. G. C. PALUMBO

Physics Department, University of Calgary, Calgary, Alberta

AND

J. A. GALT AND C. H. COSTAIN

Dominion Radio Astrophysical Observatory, Penticton, British Columbia

Received June 21, 1967

1967

Very important
result in new
hot topic

Radio pulses from extensive air showers (EAS) have been observed with a 4×4 array of dipoles polarized E-W at a center frequency of 22.25 MHz and an effective bandwidth of 4 MHz. Observations were made simultaneously with antenna beams centered 30° N and 30° S of the zenith. The magnetic dip angle being 72° , the north beam faced across the geomagnetic field lines whereas the south beam faced along the field lines. In 600 hours of observation, 1100 showers were recorded. Two 1-m^2 plastic scintillators placed 30 m apart, in coincidence, triggered the cathode-ray-oscillograph recording system.

Traces were scanned for $1\text{ }\mu\text{s}$ on either side of the expected location of the radio signals. Background levels were determined by scanning an interval of $0.75\text{ }\mu\text{s}$, $3.5\text{ }\mu\text{s}$ after the beginning of the trace. Pulses were recorded on both antenna beams. Those on the north-pointing antenna were, on the average, twice as large as those on the south-pointing one. The results suggest that while charge separation in the earth's field is more important than charge excess in generating showers, it is not dominant.

INTRODUCTION

Radio pulses from EAS have been detected since 1965 by various groups (Allan and Jones 1966; Barker *et al.* 1967; Borzhkovskii *et al.* 1966; Jelley *et al.* 1966; Porter *et al.* 1965; Vernov *et al.* 1967), the aims being to confirm the discovery, to elucidate the mechanism of emission, and to assess the prospects for detecting high-energy primary cosmic rays by radio methods.

The existence of radio pulses from EAS has been fully confirmed, but the understanding of their nature is still somewhat speculative. The suggestion by Askari'yan (1962, 1965) that a detectable radio pulse should be emitted by an EAS was based on the assumption that a negative charge excess, present in the shower front, would generate coherent emission in the metric wavelength region. Subsequently, Kahn and Lerche (1966) showed the importance of the geomagnetic deflection of the shower particles. They estimated, in a rather simplified shower model, that the trans-

effect one order of magnitude greater than the coherent Cerenkov radiation due to charge excess. Both mechanisms predict a spectrum that rises with frequency. At frequencies of the order of 100 MHz, the coherence condition is lost since the wavelength becomes comparable with the thickness of the shower front. Since the signal-to-noise ratio also improves with increasing frequency, because of decreasing galactic noise, the early measurements were made in the 40–80 MHz frequency band. More recently, unpublished work by both Colgate (1965) and Allan (1967) has suggested that the radio signals should be stronger at frequencies in the MHz range than at tens of MHz. In both cases deflections in the earth's magnetic field play an essential role.

The present experiments were undertaken to explore the feasibility of measurements at lower frequencies and to give some indication of the relative importance of the production mechanisms involving the earth's magnetic

RADIO PULSES AT 46,65 AND 110 MHz.FROM EAS.

N.Mandolesi,G.Morigi,G.G.C.Palumbo

Consiglio Nazionale delle Ricerche,TE.S.R.E.Lab.

40126 Bologna,Italy

1973

An array of 5 plastic scintillators detecting Air Showers of average size 10^6 particles has been operating in coincidence with 3 antenna arrays. The lateral distribution of radio pulses from Extensive Air Showers (EAS) has been obtained at 46, 65 and 110 MHz. At all frequencies the lateral distribution steepens quite rapidly with increasing distance from the shower core and more so at higher frequencies. A large spread of the experimental points seems to indicate fluctuations in the height of shower maximum. A frequency spectrum has been obtained from the data, for showers with core distances $75 < R < 105$ m it presents a maximum at 65 MHz. At smaller distances it seems to increase.

1. INTRODUCTION.

Since the day of their discovery (Jelley et al.1965) a lot of experimental and theoretical work has been done on radio pulses from EAS (Allan 1971a) mainly to understand the radiation mechanism in order to use radio methods to study the properties of primary cosmic radiation at very high energies. At the 12th Cosmic Ray conference at Hobart serious attempts to give quantitative information about the electric fields produced have appeared. The picture that emerges is that the lateral distribution curves of the radiation may convey valuable information about the longitudinal development of a shower.

While measurements at very low frequencies (a few MHz or less) give controversial results, measurements from a few tens of MHz up to some hundred MHz seems to be fairly consistent and reliable, although the behaviour of the radio emission for a given shower is not yet fully known. Theoretical predictions which correlate radio emission to shower parameters must be substantiated by experimental evidence before definite conclusions might be drawn on the behaviour of shower development, and from these some indications about the nature of primary Cosmic Rays.

The aim of the present work is to add experimental information to the radio lateral distribution curves and frequency dependence of the emitted radiation.

2. EXPERIMENTAL SET UP: THE "MEDICINA" SHOWER ARRAY. The site where the experiment was performed is located near the town of Medicina (~ 30 Km East of Bologna, 0 m above sea level) This site has been chosen mainly for being radio interference free. EAS are detected by 5 plastic scintillators 1 m^2 of area each. Figure 1. shows the layout of the array whose physical area is $\sim 7 \cdot 10^3 \text{ m}^2$

2005

LETTERS

Detection and imaging of atmospheric radio flashes from cosmic ray air showers

H. Falcke^{1,4,9}, W. D. Apel⁶, A. F. Badea⁶, L. Bühren⁶, K. Bekk⁶, A. Bercuci³, M. Bertina¹¹, P. L. Biermann¹, J. Blümer^{5,6}, H. Bozdog⁶, I. M. Brancus⁶, S. Buitink⁹, M. Brüggemann¹⁰, P. Buchholz¹⁰, H. Butcher⁸, A. Chisavassa¹¹, K. Daumiller⁶, A. G. de Bruyn⁶, C. M. de Vos⁶, F. Di Piero¹¹, P. Doll⁶, R. Engel⁶, H. Gemmeke⁷, P. L. Ghia¹², R. Glasstetter¹³, C. Grupen¹⁰, A. Haungs⁶, D. Heck⁶, J. R. Hörandel⁶, A. Horneffer¹, T. Huege¹, K.-H. Kampert¹³, G. W. Kant⁴, U. Klein², Y. Kolotayev¹⁰, Y. Koopman⁹, O. Krömer⁷, J. Kuijpers⁹, S. Lafebre⁹, G. Maier^{6,14}, H. J. Mathes⁶, H. J. Mayer⁶, J. Milke⁶, B. Mitrica³, C. Morello¹², G. Navarra¹¹, S. Nehls⁶, A. Nigl⁹, R. Obenland⁶, J. Oehlschläger⁶, S. Ostapchenko⁶, S. Over¹⁰, H. J. Pepping⁶, M. Petcu³, J. Petrovic⁹, S. Plewnia⁶, H. Rebe⁶, A. Risse⁸, M. Roth⁵, H. Schieler⁶, G. Schoonderbeek⁴, O. Sima³, M. Stümpert⁵, G. Toma³, G. C. Trinchero¹², H. Ulrich⁶, S. Valchierotti¹¹, J. van Buren⁶, W. van Cappellen⁶, W. Walkowiak¹⁰, A. Weindl⁶, S. Wijnholds⁴, J. Wochele⁶, J. Zabierowski¹, J. A. Zensus⁵ & D. Zimmermann¹⁰

The nature of ultrahigh-energy cosmic rays (UHECRs) at energies $>10^{19}$ eV remains a mystery¹. They are likely to be of extragalactic origin, but should be absorbed within ~ 50 Mpc through interactions with the cosmic microwave background. As there are no sufficiently powerful accelerators within this distance from the Galaxy, explanations for UHECRs range from unusual astrophysical sources to exotic string physics². Also unclear is whether UHECRs consist of protons, heavy nuclei, neutrinos or γ -rays. To resolve these questions, larger detectors with higher duty cycles and which combine multiple detection techniques³ are needed. Radio emission from UHECRs, on the other hand, is unaffected by attenuation, has a high duty cycle, gives calorimetric measurements and provides high directional accuracy. Here we report the detection of radio flashes from cosmic-ray air showers using low-cost digital radio receivers. We show that the radiation can be understood in terms of the geosynchrotron effect⁴. Our results show that it should be possible to determine the nature and composition of UHECRs with combined radio and particle detectors, and to detect the ultrahigh-energy neutrinos expected from flavour mixing^{5,6}.

When UHECRs interact with particles in the Earth's atmosphere, they produce a shower of elementary particles propagating towards the ground with almost the speed of light. The first suggestion that these air showers also could produce radio emission was made⁷ on the basis of a charge-excess mechanism, which is very strong for showers developing in solid media^{8,9}. In a couple of experimental activities in the 1960s and 1970s, coincidences between radio pulses and cosmic ray events were indeed reported^{10,11}. Owing to the limitations of electronics in those days, the measurements were cumbersome and did not lead to useful relations between radio emission and air shower parameters. As a consequence, the method was not pursued for a long time and the historic results came into question. However, the mechanism for the radio emission of air showers was recently revisited and proposed to be coherent geosynchrotron emission⁴: Secondary electrons and positrons

produced in the particle cascade rush with velocities close to the speed of light through the Earth's magnetic field and are deflected. As in synchrotron radiation, this produces dipole radiation that is relativistically beamed into the forward direction. The shower front emitting the radiation has a thickness that is comparable to (or less than) a wavelength for radio emission below ~ 100 MHz. Hence the emission is expected to be coherent to a large extent, which greatly amplifies the signal.

To see whether radio emission from cosmic rays is indeed detectable and useful in a modern cosmic ray experiment, we have built the LOPES (LOFAR Prototype Station) experiment. LOPES is a phased array of dipole antennas with digital electronics developed to test aspects of the LOFAR (Low-Frequency Array) concept. Compared to historical experiments, it provides an order of magnitude increase in bandwidth and time resolution, effective digital filtering methods, and for the first time true interferometric imaging capabilities. The radio array is co-located with the KASCADE¹² (KASCADE Shower Core and Array Detector) experiment that is now part of KASCADE-Garde at the research centre in Karlsruhe, Germany (see Supplementary Fig. 1). KASCADE provides coincidence triggers for LOPES and well-calibrated information about air shower properties. Experimental procedure and data reduction have been described by Horneffer *et al.*¹³, and we give here only a brief summary in the Methods section. A related experiment is currently under way at the Nançay radio observatory¹⁴.

Using LOPES, we have detected the radio emission from cosmic ray air showers at 43–73 MHz on a regular basis with unsurpassed spatial and temporal resolution (see Supplementary Fig. 2). After digital filtering of radio interference we still have almost the full bandwidth of $\Delta\nu = 33$ MHz available, giving us a time resolution of $\Delta t \sim 1/\Delta\nu \approx 30$ ns compared to ~ 1 μ s resolution in historic experiments. Using radio interferometric techniques we can also image the radio flash for the first time. An example is shown in Fig. 1, where the air shower is the brightest radio point source on the sky for some tens of nanoseconds (see also Supplementary Video 1). The nominal

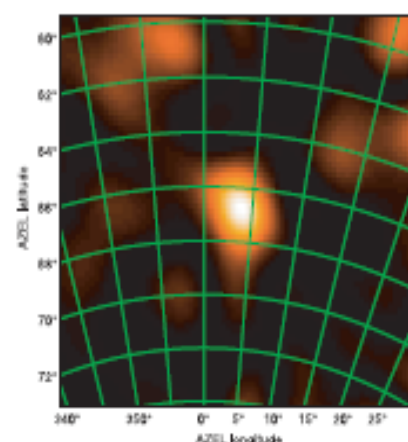


Figure 1 Radio map of an air shower. For each pixel in the map, we formed a beam in this direction integrated over 125 ns and show the resulting electric field intensity. Longitude and latitude give the azimuth and elevation (AZEL) direction (north is to the top, east to the right). The map is focused towards a distance of 2000 m (fixed curvature radius for each pixel). The cosmic ray event is seen as a bright blob of $2.4^\circ \times 1.8^\circ$ size. Most of the noise in this map is due to interference from sidelobe caused by the sparse radio array. No image deconvolution has been performed.

resolution in our maps is $\sim 2^\circ$ in azimuth and elevation towards the zenith. Within these limits the emission appears point-like. To put this in perspective, we note that previous radio experiments used fixed analogue beams with a width of $\sim 20^\circ$ and no possibilities for imaging. Current detectors for UHECRs (for example, AUGER) are limited to about $\sim 1^\circ$ accuracy. Positional accuracies for LOPES can be a fraction of a degree for bright sources. This will improve further with interferometer baselines longer than used here.

To make an initial and reliable statistical assessment of the radio properties of air showers, we have investigated a rather restrictive set of events with relatively high signal-to-noise ratio and simple selection criteria. The criteria are purely based on shower parameters reconstructed from KASCADE. Using events from the first half year of operation, starting January 2004, we selected all events with a shower

core within 70 m of the centre of LOPES, a zenith angle $<45^\circ$, and a reconstructed truncated muon number¹⁵ of $N_{\mu} > 10^{6.8} \approx 4 \times 10^6$. The truncated muon number is the reconstructed number of muons within 40–200 m of the shower core. For KASCADE, this quantity is a good tracer of primary particle energy¹⁶, $E_p \propto N_{\mu}^{0.8}$. The selection corresponds approximately to $E_p > 10^{17}$ eV. This is the upper end of the energies that KASCADE was built for. Using these selection criteria ('cuts') leaves us with 15 events and a 100% detection efficiency of the radio signal. This avoids any bias due to non-detections. The rather restrictive cut on the shower core location allows us to ignore radial dependencies. Also, the antenna gain reduces significantly at zenith angles $>45^\circ$. Even though neither KASCADE nor LOPES are optimized for large zenith angles, we have also checked for highly inclined events. Selecting all events with a much lower truncated muon number of $N_{\mu} > 10^5$ and zenith angle $>50^\circ$ we still detect $>50\%$ of all events—in many cases with very high field strengths. However, given the current uncertainties of KASCADE in shower parameters for inclined showers, we ignore those events for our analysis below.

The strength of the detected radio pulses in our sample is some μ V per m per MHz at present, but we still lack an accurate absolute gain calibration. The position of the radio flashes are coincident with the direction of the shower axis derived from KASCADE data within the errors. The average offset is $(0.8 \pm 0.4)^\circ$ as determined from our radio maps.

We find the strongest correlations between the absolute value of the electric field strength height of the pulse, ϵ and N_{μ} , and between ϵ and the geomagnetic angle, α_g . The latter is defined as the angle between the shower axis and the geomagnetic field. No obvious correlation is found with the zenith angle. Theory⁴ predicts that owing to coherence the electric field strength should scale linearly with the number of particles in the shower, which—for KASCADE—is approximately proportional to the number of muons. Hence, to first order we can separate the two effects by dividing the electric field of the radio pulse by the truncated muon number. We find that $\epsilon_p = \epsilon/N_{\mu} \propto (1 - \cos\alpha_g)$, where the lowest geomagnetic angle in the sample was $\alpha_g = 8^\circ$ (see Supplementary Fig. 3). It is also possible to use a $\epsilon_p \propto \sin\alpha_g$ behaviour, which for our data gives only marginally worse results. Simulations¹⁷ indicate that this strong dependence on α_g is largely a polarization effect, as LOPES at present currently measures only a single polarization in the east-west direction.

We can use this dependence to correct for the geomagnetic angle. Figure 2a shows the measured radio signal ϵ plotted against muon number, while Fig. 2b shows the same plot where we use a normalized field strength height, ϵ_{norm} corrected for the $(1 - \cos\alpha_g)$ dependence.

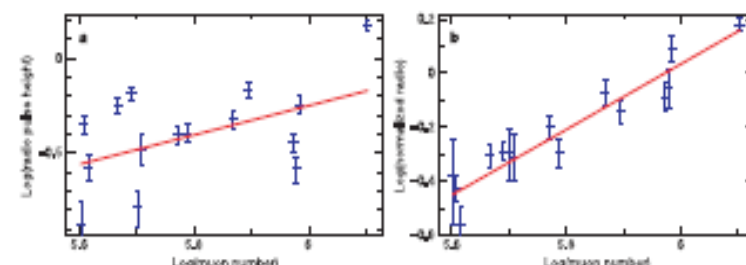


Figure 2 Radio emission as a function of muon number. **a**, The logarithm of the radio pulse height, ϵ , versus the logarithm of muon number, which has not been corrected for the geomagnetic angle dependence, α_g . As a but now the geomagnetic angle dependence is corrected for (ϵ_{norm}). The correlation

improves significantly. Solid lines indicate power-law fits. Errors were calculated from the noise in the time series before the pulse plus a nominal 5% error on gain stability. Both errors were added in quadrature. The radio pulse height units are arbitrary. Errors are one-sigma standard deviations.

¹W. Falck-Institut für Radioastronomie, 53175 Bonn, Germany. ²Radioastronomisches Institut der Universität Bonn, 53175 Bonn, Germany. ³National Institute of Physics and Nuclear Engineering, 7690 Bucharest, Romania. ⁴ASTRON, 79 90 AA Dwingelo, The Netherlands. ⁵Institut für Experimentelle Kernphysik, Universität Karlsruhe, 76021 Karlsruhe, Germany. ⁶Institut für Kernphysik, Forschungszentrum Karlsruhe, 76021 Karlsruhe, Germany. ⁷Institut für Prozessdatenverarbeitung und Elektronik, IZK, 76021 Karlsruhe, Germany. ⁸Soltan Institute for Nuclear Studies, 05050 Lodz, Poland. ⁹Department of Astrophysics, Radboud University, 6525 ED Nijmegen, The Netherlands. ¹⁰Fachbereich Physik, Universität Siegen, 57072 Siegen, Germany. ¹¹Dipartimento di Fisica Generale dell'Università, 10125 Torino, Italy. ¹²Istituto di Fisica dello Spazio Interplanetario, INFN, 10133 Torino, Italy. ¹³Fachbereich C-Raum, Universität Wuppertal, 42097 Wuppertal, Germany. ¹⁴Present address: University of Leeds, Leeds LS2 9JT, UK.

1974

A Search for Isolated Microwave Pulses from the Perseus Cluster of Galaxies

T. Delaney, G. A. Baird and H. Smith

Physics Department, University College, Dublin

J. V. Jelley and J. H. Fruin

Nuclear Physics Division, Atomic Energy Research Establishment, Harwell, Berkshire

W. P. S. Meikle and R. W. P. Drever

Department of Natural Philosophy, Glasgow University

G. Morigi and G. G. C. Palumbo

Laboratorio TESRE, Consiglio Nazionale delle Ricerche, Bologna

R. B. Partridge

Department of Astronomy, Haverford College

Received August 22, 1974

Summary. The paper describes a search for prompt microwave emissions from supernovae in the central region of the Perseus cluster of galaxies, using a coincidence technique involving five tracking radio-meters located at widely spaced sites. No coincidences were found between January and December, 1973,

and no supernovae were reported during this period from the optical surveys, in that region of sky.

Key words: supernovae — perseus cluster of galaxies — radio pulses

1. Introduction

An experiment designed to search for prompt microwave bursts from supernovae (SN) in the Coma cluster of galaxies has already been described elsewhere (Jelley *et al.*, 1974, subsequently referred to as Paper I). We present here the results from extended observations at five widely separated sites, on the central region of the Perseus cluster of galaxies, along with a calibration carried out on Solar flares.

Colgate and Noerdlinger (1971) predicted, from the original shock-wave model of supernovae (Colgate and White, 1966), that prompt bursts of radio emission would be expected from supernova explosions. LeBlanc and Wilson (1970) show, on a different model of stellar collapse, that large amounts of energy in various forms may be released in periods $\sim 0.1-3$ s. It is not however clear in this model that the energy can escape through the outer layers of the star. Our sensitivity is such that we could have detected a pulse having an energy over the entire microwave spectrum (taken arbitrarily to be 3–30 GHz) of 8.8×10^{-3} of an assumed total prompt energy release in a SN of $\sim 10^{51}$ erg, if this were at the distance of the Perseus cluster. This figure is deduced on the assumption of a flat spectrum.

Recently, isolated, intense and short bursts of X- and γ -ray emission have been discovered (Klebesadel *et al.*, 1973). The origin of these pulses have not yet been identified though on some models it has been suggested that these may arise from supernovae.

Since supernovae are rare, it is important to eliminate any spurious events without significantly increasing the energy threshold of the system. This was achieved by using a coincidence technique, and in this experiment five widely spaced stations were used.

The general arguments for using microwave frequencies as opposed to VHF have been outlined already in Paper I, but may be summarised as follows: (1) the absorption and dispersion in a plasma at microwave frequencies is considerably less than at VHF. (2) the interference from the Sun is negligible and sources of man-made interference are also much less severe; Furthermore, several searches for isolated radio pulses have already been carried out in the VHF and UHF bands (e.g. Smith, 1950; Charman *et al.*, 1970; Colgate *et al.*, 1972; Huguenin and Moore, 1974).

The intrinsically low rate of occurrence of supernovae from individual galaxies necessitated choosing large clusters for the purpose of these experiments.

1975

A REVIEW OF SOME RADIO AND MICROWAVE
SEARCHES FOR TRANSIENT PHENOMENA IN
RELATION TO VELA GAMMA-RAY BURSTS
AND SUPERNOVAE*

G. A. BAIRD

Physics Department, University College, Dublin, Ireland

W. P. S. MEIKLE

Department of Natural Philosophy, University of Glasgow, Scotland

J. V. JELLEY

Nuclear Physics Division, Atomic Energy Research Establishment, Harwell, England

G. G. C. PALUMBO

T.E.S.R.E. LAB. C.N.R. Via De Castagnoli 1, Bologna, Italy

R. B. PARTRIDGE

Dept. of Astronomy, Haverford College, Haverford, Pennsylvania, U.S.A.

(Received 18 August, 1975)

Abstract. Radio systems with all sky viewing antennas at 151 MHz were operating at 5 widely spaced stations over the period 1970–1973, during which 19 Vela γ -ray bursts were detected. The records were analysed for each Vela time but no radio coincidences were recorded. A new experiment in the radio band operating at 408 MHz with similar objectives is now under construction and will be described.

Five radiometers at 10 GHz have been tracking the Perseus cluster of galaxies for over one year. The supernova reported on 1 March in Perseus occurred during our observing time but failed to give evidence from prompt emission in excess to 8×10^{-13} erg cm $^{-2}$ event $^{-1}$, for event durations 0.3–100 s.

Since early 1970 an almost continuous series of experiments have been carried out to search for single isolated pulses of radio emission from various astronomical objects (Table I). The basic radio system, at each of the sites involved in the experiment, consisted of a 151 MHz interferometer with either single dipoles for all-sky viewing or multi-element ladder arrays for directional studies and have been discussed elsewhere (ref. in Table I). In addition to this basic system, several stations operated interferometers at other frequencies, also for extended periods. The authenticity of a pulse was tested by searching for a similar coincident pulse in the records of the other stations and, in the original experiments, by studying only night-time data in order to limit the effect of solar emissions. The integration time constants were typically of the order of 1 s and the coincidence resolving time between stations was of the order of

* Paper presented at the COSPAR Symposium on Fast Transients in X- and Gamma-Rays, held at Varna, Bulgaria, 29–31 May, 1975.

1977

UPPER LIMITS FOR THE MICROWAVE PULSED EMISSION FROM SUPERNOVA EXPLOSIONS IN CLUSTERS OF GALAXIES

G. G. C. PALUMBO, N. MANDOLESI and G. MORIGI

T.E.S.R.E., LAB/C.N.R., Bologna, Italy

G. A. BAIRD and T. DELANEY

Dept. of Physics, University College, Dublin, Ireland

W. P. S. MEIKLE and R. W. P. DREVER

Dept. of Natural Philosophy, University of Glasgow, Glasgow, U.K.

J. V. JELLEY and J. H. FRUIN

Nuclear Physics Division, A.E.R.E., Harwell, U.K.

and

R. B. PARTRIDGE

Dept. of Astronomy, Haverford College, Haverford, Pennsylvania, U.S.A.

(Received 4 October, 1977)

Abstract. Between 1972 and 1975 an international collaborative search was carried out for prompt 10 GHz emission at the onset of supernovae. The motivations and techniques involved in this effort are described, and the results of the three years' work are summarized. No pulses from supernovae were detected, the best upper limit being 4×10^{43} ergs in a 40 MHz band at 10 GHz for a pulse time-scale ≤ 0.5 s. Methods for improving this limit are briefly described.

1. Introduction

The discovery of pulsars started a new chapter of experimental astrophysics which, recently, has been named 'short-time constant astrophysics'. This new field includes a variety of phenomena such as bursters (mostly in the X- and gamma-ray energy range), the unexplained gamma-ray bursts, and in general all those fast transient phenomena (FTP) which take place during astrophysical events in times which are short compared to the time of observation (Bondi, 1970; Cavallo, 1973).

Supernova (SN) explosions are of considerable astrophysical interest for many reasons. To begin with they are among the most violent phenomena in nature. Up to 10^{50} erg can be released in explosions which, optically, last some 10^6 s; the luminosity of a SN being some $10^9 L_{\odot}$, i.e. of brightness comparable to the Galaxy in which it takes place. It has been well known for many years that while the time-scale of stellar collapse involving stellar envelopes may last from minutes to hours or days, core collapse can be of the order of a few seconds and as short as milliseconds for densities ranging from white dwarf to neutron star densities. The physical processes involved in such phenomena are obviously of great importance in understanding the late stages

2009

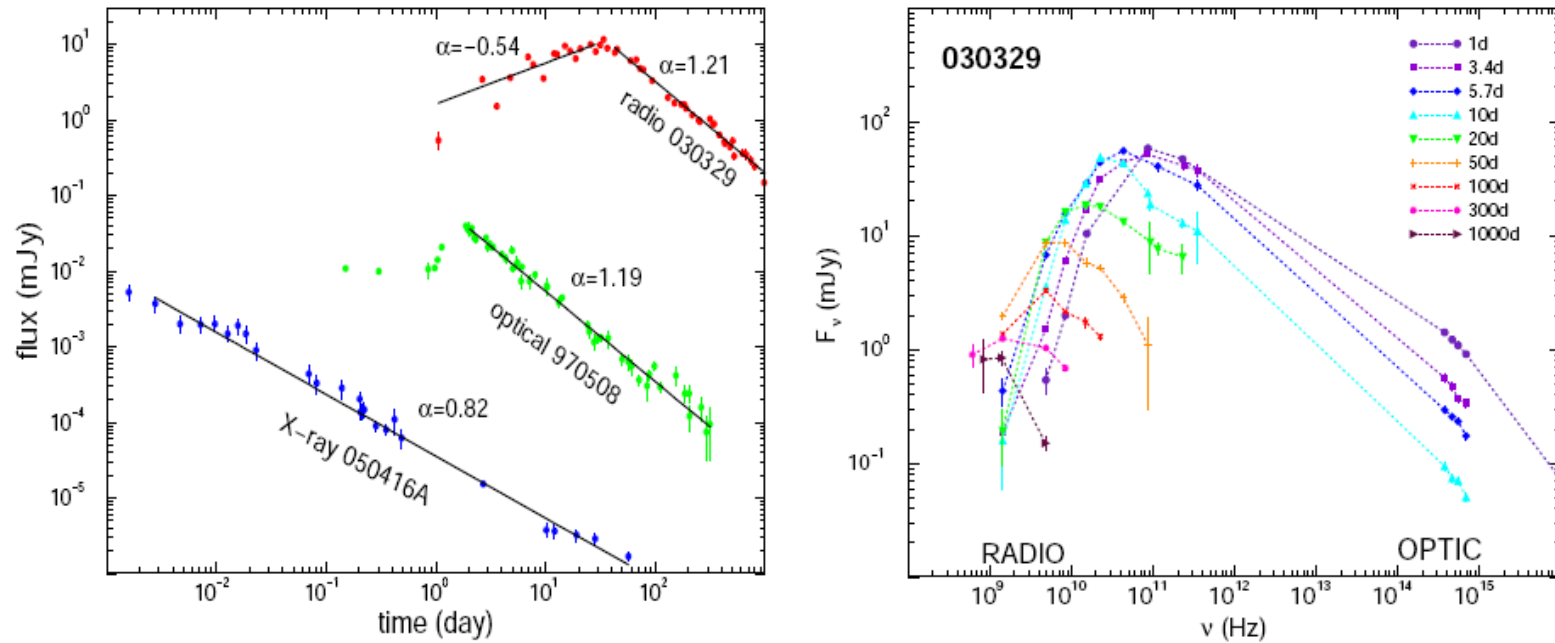


FIGURE 3. *Left panel:* examples of radio, optical, and X-ray afterglows displaying long-lived flux power-law decays. The radio flux of GRB afterglow 030329 is affected by scintillation, which quenches after few tens of days. The optical light-curve of GRB afterglow 970508 displayed an unusual, late rise at 1–2 days. *Right panel:* evolution of the radio-to-optical spectrum of GRB afterglows 030329, showing its gradual softening (decreasing peak energy) and dimming (decrease of peak flux). Color coding used indicates earlier times with bluer colors and later times with redder colors.

1974

Very Important
result and may
have forced early
publication of Vela
GRBs

OBSERVATION OF A CELESTIAL HARD X-RAY BURST IN COINCIDENCE WITH A GAMMA-RAY BURST

G. G. C. PALUMBO, G. FERRICINI, AND G. R. VESPIGNANI
Lab.TE.S.R.E./C.N.R., Bologna, Italy

Received 1973 December 6; revised 1974 January 24

ABSTRACT

One of the celestial γ -ray bursts recently discovered by the Vela satellites has been observed in the 27–189 keV energy range by a directional X-ray detector aboard OSO-6, on 1969 October 7. The event has an intensity of about 10^{-4} ergs cm^{-2} in the 50–200 keV energy range. It seems to start earlier but reaches its maximum in correspondence to the Vela time and is located at high northern galactic latitude. The 3σ positional error box is, in fact, centered at $\alpha = 12^{\text{h}}19^{\text{m}}$, $\delta = +30^\circ$. Possible spectral shapes are also discussed.

Subject headings: gamma rays — X-rays

I. INTRODUCTION

The recently discovered cosmic γ -ray bursts were first observed by means of omnidirectional detectors aboard the Vela 3A, 5B, 6A, 6B satellites (Klebesadel, Strong, and Olson 1973). From the positions of the spacecrafts and arrival times of the bursts their possible directions were limited either to a cone or to the intersection of two cones in the best cases. Of the Vela events, six have been confirmed by observations from IMP-6 (Cline *et al.* 1973), and their spectra have been measured between 100 and 1200 keV. One of these has also been measured down to 7 keV by the UCSD experiment on OSO-7 and located in a 4° radius 90 percent error circle (Wheaton *et al.* 1973). We report here on the observation of a hard X-ray burst coincident with one Vela event.

II. OBSERVATIONS

Data for this measurement were available from the Bologna wheel experiment aboard the OSO-6 satellite in the 27–189 keV energy range.

Instrumental characteristics and data analysis have been described elsewhere (Brini *et al.* 1971; Brini *et al.* 1973). The detector is a 5 cm^2 NaI(Tl) scintillator, collimated to a $18^\circ \times 23^\circ$ FWHM directional response. The narrower dimension of the response lies on the wheel scan plane (azimuthal plane).

A list of 19 Vela events with their times of arrival was made available to us by Dr. I. R. Strong (1973). Thirteen of them, including one of solar origin, occurred during the operational life of OSO-6.

Corresponding to each of the quoted times, data have been searched over a period of a few minutes. One burst was found at about 0726 UT, 1969 October 7, when no reported solar activity was in progress and the spacecraft was away from the regions of charged-particle interference. Its position along the scan plane was at $\sim 36^\circ$ from the Sun and at $\sim 70^\circ$ from the horizon. The temporal profile of count rates from 49 to 189 keV

in a 20° azimuthal sector, in figure 1, outlines an event lasting well over 1 minute, starting earlier but corresponding with the time of the Vela γ -ray burst ($07^{\text{h}}26^{\text{m}}31^{\text{s}}$) at the peak of intensity. Each time section is an average over 15.36 s elapsed time corresponding to ~ 0.72 s observation time per 20° sector and about 7.5 satellite rotations; 2.4 s are lost in discharging the counter registers.

A background has been estimated by averaging the count rate in a 40° azimuthal sector centered on the peak position, immediately before and after the appearance of the burst, for a total of 2 minutes of time.

The excess count rates in the four energy channels are also plotted in figure 1, for the time interval of maximum intensity 20° around the peak. Best fits of these data for three adopted spectral shapes dn/dE , namely, $E^{-\alpha}$, $\exp(-E/E_0)$, $E^{-1} \exp(-E/E_0)$, were computed on the three highest energy channels only. The first channel, which normally has a higher instrumental background, was saturated.

Based on the χ^2 goodness of fit, a power-law spectrum appears to be slightly more suitable in three time intervals (see table 1). No corrections for secondary effects have, however, been applied.

An estimate of energy output over the burst duration gives about 10^{-4} ergs cm^{-2} between 50 and 200 keV. While all the IMP-6 spectra agree with an exponential shape above 100 keV, the only other spectrum known

TABLE 1
BEST-FIT SPECTRAL SHAPES FOR X-RAY BURST

Time (UT)	dn/dE					
	$E^{-\alpha}$		$\exp(-E/E_0)$		$E^{-1}\exp(-E/E_0)$	
	α	χ^2	$E_0(\text{keV})$	χ^2	$E_0(\text{keV})$	χ^2
07 ^h 26 ^m 00 ^s ..	3.5 ± 1.2	0.30	17 ± 9	0.65	26 ± 16	0.53
07 26 30 ..	2.7 ± 0.7	0.90	27 ± 10	1.96	45 ± 24	1.60
07 26 45 ..	5.8 ± 2.8	0.93	8 ± 7	0.99	10 ± 9	0.99

1975

GAMMA-RAY BURSTS OBSERVED BY A HARD X-RAY EXPERIMENT ABOARD OSO-6

G. PIZZICCHINI, G. G. C. PALUMBO, AND A. SPIEZICHINO

Laboratorio di Tecnologie e Studio delle Radiazioni Extraterrestri, Consiglio Nazionale delle Ricerche, Bologna, Italy

Received 1974 August 15

ABSTRACT

The data of the Bologna hard X-ray experiment aboard the OSO-6 satellite have been searched for events in coincidence with the 14 cosmic γ -ray bursts reported by Strong, Klebesadel, and Olson which occurred during the OSO-6 lifetime (1969 August to 1972 January). Three events have been detected. The first one (69-2) was discussed in a previous paper. We report here on the other two events (71-6 and 71-3) and give the information that could be deduced from our data about the remaining 11 *Vela* events which were not detected. For some of these events it has been possible to exclude one of the *Vela* positions.

Subject headings: gamma-ray bursts — X-rays — X-ray sources

1. INTRODUCTION

The data from the Bologna hard X-ray experiment (27–189 keV) flown aboard the OSO-6 satellite have been searched for X-ray bursts in coincidence with the γ -ray bursts observed by the *Vela* satellites, whose catalog has recently been published (Strong, Klebesadel, and Olson 1974).

The hard X-ray detector was a 5 cm² NaI(Tl) scintillator, collimated to 18° \times 23° FWHM directional response and with four energy channels (27–49–75–118–189 keV). Instrumental and satellite characteristics as well as data analysis procedures have been described in detail elsewhere (Brini *et al.* 1971; Brini *et al.* 1973).

The OSO-6 lasted from 1969 August to 1972 January. In this period 15 γ -ray bursts were detected by the *Vela* satellites as reported by Strong *et al.* (1974). Event 70-1 of solar origin was clearly seen in our detector, but it is omitted here. For events 71-2 and 72-1 no data are available.

The results for event 69-2 have been discussed in a previous *Letter* (Palumbo, Pizzichini, and Vespignani 1974). We report here on the remaining 11 events, two of which, 71-6 and 71-3, were detected.

II. OBSERVATIONS AND RESULTS

In table 1 we have summarized the γ -ray bursts seen by *Vela* for which OSO-6 data exist and, for comparison, the information so far collected, to our knowledge, by various observers. The event order is kept as given by Strong *et al.* (1974) in their catalog.

Our apparatus was located on the rotating wheel of the satellite so that it scanned a strip of sky with a 2-s period. If a source lay in that strip and the burst was long enough, we could see a directional peak, hence not only detect the burst but determine the source location. This is what happened for event 69-2 (Palumbo *et al.* 1974).

On the other hand, since the radiation was so energetic, some of it, however absorbed and degraded, could leak through the shield and the satellite material. The sensitivity due to this indirect mechanism was, of

course, lower but still allowed detection of the most intense events. The other two bursts, i.e., 71-6 and 71-3, were in fact seen as a general increase in the counting rate, independent of direction. Their observed durations \sim 8 s and \sim 12 s, respectively, are in agreement with NRL (OSO-6) data. Since we detected the secondary products of more energetic photons interacting with the shielding material surrounding the detector, this duration should refer to energies higher than ours.

At our energies, event 69-2 appears to be much longer than the corresponding *Vela* event and exhibits, in fact, a precursor, in agreement with what has been reported by Kane, Mahoney, and Anderson (1974) and Share, Meekins, and Kreplin (1974) at about the same energies. This different behavior is reflected in the measured spectra (figs. 2b and 2c) which appear to be much flatter than the one obtained for 69-2, where the primary radiation was observed (fig. 2d). Event 71-6 was detected at \sim 7 σ (fig. 2a). No *Vela* positions or cone are available, and the only excluded regions are the Earth's zone and the sky strip scanned by the detector (fig. 1c). Event 71-3 (figs. 1d and 2a) was detected by our instrument at \sim 8 σ . If the source were in the field of view (*Vela* position $\delta^1 = 283^\circ$, $\delta^1 = -22^\circ$), a peak as for event 69-2 should have been observed. But since the increase in counting rate is independent of the instrument line of sight, our data therefore favor the other position ($\delta^1 = 185^\circ$, $\delta^1 = -22^\circ$).

There are a number of *Vela* events which our instrument did not detect. For these events we made the following assumptions: (a) If the source was outside the field of view, we assumed that all events which, according to the *Vela* catalog, had fluxes and durations comparable or greater than those of 71-6 and 71-3 were detectable, whereas events comparable or smaller than 70-3 were below threshold. (b) If the source was in the field of view, much weaker events could be seen but only if they lasted longer than the satellite's rotation period (2 s).

Clearly, the possibility of detecting a burst depended also on the background, which was not constant; anyway, it was lower than for event 71-3 for all other *Vela* times.

2008

ARTICLES

Broadband observations of the naked-eye γ -ray burst GRB 080319B

J. L. Racusin¹, S. V. Karpov², M. Sokolowski³, J. Granot⁴, X. F. Wu^{1,5}, V. Pal'shin⁶, S. Covino⁷, A. J. van der Horst⁸, S. R. Oates⁹, P. Schady⁹, R. J. Smith¹⁰, J. Cummings¹¹, R. L. C. Starling¹², L. W. Piotrowski¹³, B. Zhang¹⁴, P. A. Evans¹², S. T. Holland^{15,16,17}, K. Malek¹⁸, M. T. Page⁹, L. Vetere¹, R. Margutti¹⁹, C. Guidorzi²⁰, A. P. Kambale²⁰, P. A. Curran²⁰, A. Beardmore¹², C. Kouveliotou²¹, L. Mankiewicz²², A. Melandri¹⁰, P. T. O'Brien¹², K. L. Page¹², T. Piran²³, N. R. Tanvir¹², G. Wrochna²⁴, R. L. Aptekar²⁵, S. Barthelmy¹¹, C. Bartolini²⁶, G. M. Beskin²⁷, S. Bondar²⁸, M. Bremer²⁹, S. Campana⁷, A. Castro-Tirado³⁰, A. Cucchiara¹, M. Cwik¹³, P. D'Avanzo³¹, V. D'Elia³², M. Della Valle^{33,34}, A. de Ugarte Postigo³⁰, W. Dominik¹³, A. Falcone¹, F. Fiore²⁷, D. B. Fox¹, D. D. Frederiks³⁵, A. S. Fruchter³¹, D. Fugazza², M. A. Garrett^{32,33,34}, N. Gehrels¹¹, S. Golovetski³⁶, A. Gomboc³⁵, J. Gorosabel³⁶, G. Greco²³, A. Guarnieri²³, S. Immler^{15,17}, M. Jelinek³⁶, G. Kasprzowicz³⁶, V. LaParola³⁷, A. J. Levan³⁸, V. Mangano³⁷, E. P. Mazets³⁹, E. Molinari², A. Moretti², K. Nawrocki⁴⁰, P. P. Oleynik⁴¹, J. P. Osborne¹², C. Pagani¹, S. B. Pandey³⁹, Z. Paragi⁴⁰, M. Perri⁴¹, A. Piccioni¹², E. Ramirez-Ruiz⁴², P. W. A. Roming¹, I. A. Steele¹⁰, R. G. Strom^{30,32}, V. Testa³⁷, G. Tosti⁴³, M. V. Ulanov⁴⁴, K. Wiersema¹², R. A. M. J. Wijers²⁰, J. M. Winters²⁵, A. F. Zarnack⁴⁵, F. Zerbi⁴⁶, P. Mészáros⁴⁴, G. Chincarini^{7,19} & D. N. Burrows¹

Long-duration γ -ray bursts (GRBs) release copious amounts of energy across the entire electromagnetic spectrum, and so provide a window into the process of black hole formation from the collapse of massive stars. Previous early optical observations of even the most exceptional GRBs (990123 and 030329) lacked both the temporal resolution to probe the optical flash in detail and the accuracy needed to trace the transition from the prompt emission within the outflow to external shocks caused by interaction with the progenitor environment. Here we report observations of the extraordinarily bright prompt optical and γ -ray emission of GRB 080319B that provide diagnostics within seconds of its formation, followed by broadband observations of the afterglow decay that continued for weeks. We show that the prompt emission stems from a single physical region, implying an extremely relativistic outflow that propagates within the narrow inner core of a two-component jet.

The GRB 080319B, discovered by NASA's Swift GRB Explorer mission¹ on 19 March 2008, set new records among these most luminous transient events in the Universe. GRBs are widely thought to occur through the ejection of a highly relativistic, collimated outflow (jet),

produced by a newly formed black hole. Under the standard fireball model^{2,4}, collimated relativistic shells propagate away from the central engine, crash into each other (internal shocks) and decelerate as they plough into the surrounding medium (external forward

shocks). Reverse shocks propagate back into the jet, generating optical emission. With a uniquely bright peak visual magnitude of 5.3 (Fig. 1) at a redshift of $z = 0.937$ (ref. 7), GRB 080319B was the brightest optical burst ever observed. An observer in a dark location could have seen the prompt optical emission with the naked eye. The astronomical community has been waiting for such an event for the past nine years, ever since GRB 990123 (the previous record holder for the highest peak optical brightness) peaked at a visual magnitude of ~ 9 , leading to significant insight into the GRB optical emission mechanisms⁸.

The location of GRB 080319B was fortuitously only $10''$ away from GRB 080319A, detected by Swift less than 30 min earlier, allowing several wide-field telescopes to detect the optical counterpart of GRB 080319B instantly. The rapid localization by Swift enabled prompt multi-wavelength follow-up observations by robotic ground-based telescopes, resulting in arguably the best broadband GRB observations obtained so far. These observations continued for weeks afterwards as we followed the fading afterglow, providing strong constraints on the physics of the explosion and its aftermath.

At its peak, GRB 080319B displayed the brightest optical and X-ray fluxes ever measured for a GRB, and one of the highest γ -ray fluences recorded. Our broadband data cover 11.5 orders of magnitude in wavelength, from radio to γ -rays, and begin (in the optical and γ -ray bands) before the explosion. We identify three different components responsible for the optical emission. The earliest data (at $t = T_0 - T_0 < 50$ s) provide evidence that the bright optical and γ -ray emissions stem from the same physical region within the outflow. The second optical component (50 s $< t < 800$ s) shows the distinct characteristics of a reverse shock, and the final component

(at $t > 800$ s) represents the afterglow produced as the external forward shock propagates into the surrounding medium. Previous measurements of GRBs have revealed one or two of these components at a time^{9–11}, but never all three in the same burst with such clarity. GRB 080319B is therefore a testbed for broad theoretical modelling of GRBs and their environments.

Discovery and broadband observations

Swift's Burst Alert Telescope (BAT¹²; 15–30 keV) triggered¹³ on GRB 080319B at $T_0 = 06:12:49$ UT on 19 March 2008. The burst was detected simultaneously with the Konus γ -ray detector (20 keV to 15 MeV) on board the Wind satellite^{14,15}. Both the BAT and Konus-Wind (KW) light curves (Supplementary Figs 1 and 3) show a complex, strongly energy-dependent structure, with many clearly separated pulses above 70 keV and a generally smoother behaviour at lower energies, lasting ~ 57 s.

The wide-field robotic optical telescope 'Pi of the Sky'¹⁶ and the wide-field robotic instrument Telescopio Optimizzatore per la Ricerca dei Transienti Ottici Rapidi (TORTORA¹⁷) both serendipitously had the GRB within their fields of view at the time of the explosion (as they were both already observing GRB 080319A (ref. 18)). 'Pi of the Sky' observed the onset of the bright optical transient, which began at 2.75 ± 5 s after the BAT trigger, rose rapidly, peaked at $\sim T_0 + 18$ s and then faded below the threshold to magnitude ~ 12 after 5 min. TORTORA measured the brightest portion of the optical flash with high time resolution, catching three apparent peaks (Fig. 1) and enabling us to do detailed comparisons between the prompt optical and γ -ray emissions.

The Swift spacecraft and the Rapid Eye Mount (REM¹⁸) telescope both initiated automatic slews to the burst, resulting in optical observations with REM and the Swift Ultraviolet-Optical Telescope (UVOT¹⁹), and X-ray observations with the Swift X-ray Telescope (XRT²⁰). Over the next several hours we obtained ultra-violet, optical and near-infrared (NIR) photometric observations of the GRB afterglow with the Swift-UVOT, REM, the Liverpool Telescope, the Faulkes Telescope North, Gemini-North, and the Very Large Telescope. Subsequent optical spectroscopy by Gemini-N and the Hobby-Eberly Telescope confirmed the redshift of 0.937 (Supplementary Figs 4 and 5). A millimetre-wavelength counterpart was detected with the IRAM Plateau de Bure Interferometer at $\sim T_0 + 16$ h. Multiple epochs of radio observations with the Westerbork Synthesis Radio Telescope revealed a radio counterpart ~ 2 –3 days after the burst. X-ray and optical observations continued for more than four weeks after the burst. The composite broadband light curves of GRB 080319B, which include all data discussed throughout this paper, and cover eight orders of magnitude in flux and more than six orders of magnitude in time, are shown in Fig. 2 and summarized in Table 1. All of these data are given in Supplementary Information.

Ultra-relativistic prompt emission

The contemporaneous bright 'optical flash' and the γ -ray burst (Fig. 1) provide important constraints on the nature of the prompt GRB emission mechanism. Although there is a general consensus that the prompt γ -rays must arise from internal dissipation within the outflow, probably as a result of internal shocks, the optical flash may arise either from the same emitting region as the γ -rays or from the reverse shock that decelerates the outflow as it sweeps up the external medium. The reverse shock becomes important when the inertia of the swept-up external matter starts to slow down the ejecta appreciably, at a larger radius than the dissipation by internal shocks.

The temporal coincidence of the onset and overall shape of the prompt optical and γ -ray emissions suggest that both originate from the same physical region (see also refs 22, 23), although their respective peaks during this phase do not positively correlate in detail (see Supplementary Figs 8–10 and the related discussion in Supplementary Information). Nevertheless, the initial steep rise (at

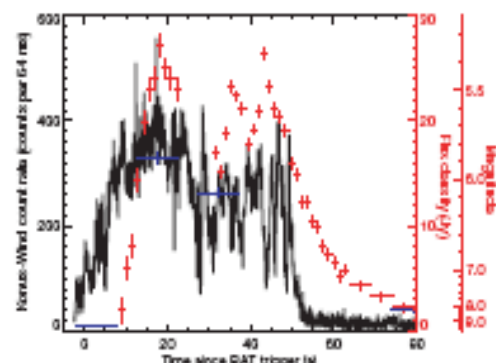


Figure 1 | Light curve of prompt emission. The Konus-Wind background-subtracted γ -ray light curve (black; 16–160 keV), shown relative to the trigger time T_0 of the Swift-BAT. The burst had a peak γ -ray flux of $F_\gamma = (2.26 \pm 0.21) \times 10^{-5} \text{ erg cm}^{-2} \text{ s}^{-1}$, a fluence $F_\gamma (20 \text{ keV to } 7 \text{ MeV})$ of $(6.23 \pm 0.13) \times 10^{-4} \text{ erg cm}^{-2}$, a peak isotropic equivalent luminosity $L_{\text{iso}} = (1.01 \pm 0.09) \times 10^{49} \text{ erg s}^{-1}$ (at the luminosity distance d_L of $1.9 \times 10^{28} \text{ cm}$, assuming cosmological parameters $H_0 = 71 \text{ km s}^{-1} \text{ Mpc}^{-1}$, $\Omega_m = 0.27$ and $\Omega_\Lambda = 0.73$), and an isotropic equivalent γ -ray energy release $E_{\text{iso}} = (1.3 \pm 0.1) \times 10^{51} \text{ erg}$ (20 keV to 7 MeV). These are among the highest measured so far. Optical data from 'Pi of the Sky' (blue) and TORTORA (red) are superimposed for comparison. The optical emission begins within seconds of the onset of the burst. The TORTORA data have a gap during the slew of the REM telescope onto this field, but show three sub-peaks in the optical brightness, reaching a peak brightness of 5.3 mag (white). The γ -ray light curve has multiple short peaks; these are not positively correlated with the optical peaks in detail (compare with ref. 23). If the synchrotron self-absorption frequency is slightly above the optical emission, this may account for the broad optical pulse and the lack of detailed correlation. However, the optical flash begins and ends at about the same time, providing strong evidence that both originate at the same site. See Supplementary Information for a more detailed description of correlation tests. All plotted error bars are 1 σ , and quoted parameter errors are 90% confidence.

¹Department of Astronomy and Astrophysics, 525 Casey Laboratory, Pennsylvania State University, University Park, Pennsylvania 16802, USA. ²Special Astrophysical Observatory, Nizhniy Arkhyz, Zelenchukskiy region, Karachai-Cherkess Republic, Russia 369167. ³Soltan Institute for Nuclear Studies, 05-400 Otwock-Swiedry, Poland. ⁴Centre for Astrophysics Research, University of Hertfordshire, College Lane, Hatfield AL9 9AB, UK. ⁵Purple Mountain Observatory, Chinese Academy of Sciences, Nanjing 210008, China. ⁶Yale Physics-Tech Institute, Laboratory for Experimental Astrophysics, Saint Petersburg 194 021, Russian Federation. ⁷INAF-Osservatorio Astronomico di Brera, via E. Bianchi 46, I-220 07 Merate (LC), Italy. ⁸NASA Postdoctoral Program Fellow, NASA/C, 320 Spauldin Drive, Huntsville, Alabama 35895, USA. ⁹The UCL Mull and Space Science Laboratory, Holmbury St Mary, Surrey RH8 6HT, UK. ¹⁰Astrophysics Research Institute, Liverpool John Moores University, Twelve Quays House, Birkenhead CH41 3LD, UK. ¹¹Astrophysics Science Division, Code 660, NASA's Goddard Space Flight Center, 8800 Greenbelt Road, Greenbelt, Maryland 20771, USA. ¹²Department of Physics and Astronomy, University of Leicester, LE1 7RH, UK. ¹³Institute of Experimental Physics, University of Warsaw, Hoza 69, 00-681 Warsaw, Poland. ¹⁴Department of Physics and Astronomy, University of Nevada Las Vegas, Las Vegas, Nevada 89154, USA. ¹⁵Astrophysics Science Division, Code 6603, NASA's Goddard Space Flight Center, 8800 Greenbelt Road, Greenbelt, Maryland 20771, USA. ¹⁶Universities Space Research Association, 10271 Wilcox Circle, Suite 300, Columbia, Maryland 21044, USA. ¹⁷Centre for Research and Exploration in Space Science and Technology, Code 660, NASA's Goddard Space Flight Center, 8800 Greenbelt Road, Greenbelt, Maryland 20771, USA. ¹⁸Centre for Theoretical Physics, PAF, Al. Lotników 32/46, 02-660 Warsaw, Poland. ¹⁹Universitat de València, Institut de Física d'Altes Energies, Departament de Física, Campus de Burjassot, 46100 Burjassot, Spain. ²⁰Department of Physics, University of Amsterdam, Kruislaan 403, 1098 SJ Amsterdam, The Netherlands. ²¹NASA Marshall Space Flight Center, VP02, NASA/C, 320 Spauldin Drive, Huntsville, Alabama 35895, USA. ²²Racal Institute for Physics, The Hebrew University, Jerusalem 91904, Israel. ²³Università di Bologna, Via S. Zaccaria 1, 40126 Bologna, Italy. ²⁴Institute for Experimental and Theoretical Physics, 36-197, Russian Federation. ²⁵Institute de Radioastronomie Millimétrique (IRAM), 300 rue de la Piscine, 38406 Saint Martin d'Hères, France. ²⁶Instituto de Astrofísica de Andalucía (IAA-CSIC), PO Box 3004, 180 08 Granada, Spain. ²⁷INAF - Osservatorio Astronomico di Roma, via di Cassini 167, 00190 Monteporzio Catone, Italy. ²⁸European Southern Observatory, Karl-Schwarzschild-Strasse 2, D-85748 Garching bei München, Germany. ²⁹INAF - Osservatorio Astronomico di Capodimonte, S. Maria Maggiore, 36, 80131 Napoli, Italy. ³⁰European Southern Observatory, Casla 19001, Santiago 19, Chile. ³¹Space Telescope Science Institute, 3700 San Martin Drive, Baltimore, Maryland 21208, USA. ³²Netherlands Institute for Space Astronomy (ASTRON), Postbus 27990 AA Dwingelo, The Netherlands. ³³Leiden Observatory, University of Leiden, PO Box 1300, Leiden 2300 RA, The Netherlands. ³⁴Centre for Astrophysics and Supercomputing, Swinburne University of Technology, Hawthorn, Victoria 3122, Australia. ³⁵School of Mathematics and Physics, University of Ljubljana, Jadranska 19, SI-1000 Ljubljana, Slovenia. ³⁶Institute of Electronic Systems, Warsaw University of Technology, Koszykowa 75/79, 00-665 Warsaw, Poland. ³⁷INAF - IASF IN, Via Ugo la Motta 151, 00146 Roma, Italy. ³⁸Department of Physics, University of Warwick, Coventry CV4 7AL, UK. ³⁹Astronomy Research Institute of Observational Sciences (AROS), Maroon Peak, Haleakala, Maui, Hawaii 20709, USA. ⁴⁰Joint Institute for VLBI in Europe (JIVE), Postbus 2, 7900 AA Dwingelo, The Netherlands. ⁴¹AGI Science Data Center, c/o ISSRI, via G. Galilei, 00044 Frascati, Italy. ⁴²Department of Astronomy and Astrophysics, University of California, Santa Cruz, California 95064, USA. ⁴³University of Perugia, Piazza della Università 1, 06100 Perugia, Italy. ⁴⁴Physics Department, 104 Casey Laboratory, Pennsylvania State University, University Park, Pennsylvania 16802, USA.

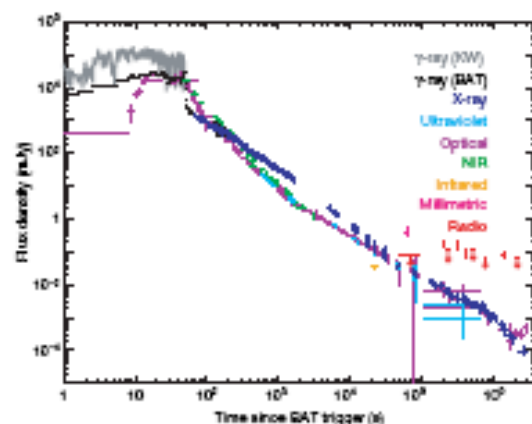


Figure 2 | Composite light curve. Broadband light curve of GRB 080319B, including radio, millimetric, infrared, NIR, optical, ultraviolet, X-ray and γ -ray flux densities. The ultraviolet, optical and NIR data are normalized to the UVOT v -band in the interval between $T_0 + 1,500$ s and $T_0 + 10$ ks. The Swift-BAT data are extrapolated down into the XRT bandpass (0.3–10 keV) for direct comparison with the XRT data. The combined X-ray and BAT data are scaled up by a factor of 4.5, and the Konus-Wind (KW) data are scaled up by a factor of 10^3 for comparison with the optical flux densities. This figure includes our own data, plus one VLA radio data point⁴⁰, and optical data from the Katzman Automatic Imaging Telescope, Nickel and Gehrels³⁹. The deviations in the NIR points from $T_0 + 100$ s to $T_0 + 600$ s are due to strong colour evolution in the spectral energy distributions at this time; these points were not included in our overall light-curve fit (Supplementary Fig. 6). After the optical flash, the optical light curve is best described by the superposition of three different power-law components (Supplementary Fig. 6) with decay indices of $\alpha_{\text{opt},1} = 6.5 \pm 0.9$ (the tail of the optical flash), $\alpha_{\text{opt},2} = 2.49 \pm 0.09$ and $\alpha_{\text{opt},3} = 1.25 \pm 0.02$. The X-ray light curve clearly differs from the optical light curve during the first ~ 12 h. After a short flat smooth transition from the tail of the γ -ray prompt emission, the X-ray light curve (Supplementary Fig. 7) after ~ 60 s can be fitted by a triple broken power-law function with decay indices of 1.44 ± 0.07 , 1.85 ± 0.10 , $1.17^{+0.33}_{-0.23}$ and $2.61^{+0.60}_{-0.50}$, and with break times of $2,262 \pm 940$ s, $4.1^{+2.8}_{-1.5} \times 10^4$ s and $(1.0 \pm 0.5) \times 10^5$ s ($\chi^2/\text{d.o.f.} = 880/697 = 1.26$), or by the superposition of two broken power-laws with decay indices of 1.45 ± 0.05 , $2.05^{+0.44}_{-0.35}$, $0.95^{+0.28}_{-0.24}$ and $2.70^{+0.46}_{-0.35}$, and break times of $2,800^{+1,000}_{-1,200}$ s and $9.5^{+2.0}_{-1.1} \times 10^4$ s ($\chi^2/\text{d.o.f.} = 902/701 = 1.29$). All plotted error bars are 1σ , and quoted parameter errors are 90% confidence.

$t < 18$ s), the rapid decline (at $t > 43$ s) and the constant optical pulse widths indicate^{34,35} that the optical flash did not arise from a reverse shock (compare with GRB 990123; refs 27, 28).

The flux density of the optical flash is $\sim 10^4$ times larger than the extrapolation of the γ -ray spectrum into the optical band (Fig. 3). The popular interpretation of the soft γ -rays as synchrotron emission cannot account for such a bright optical component from the same physical region, suggesting that different radiation mechanisms must dominate in each spectral regime. The most natural (but by no means the only viable) candidates are synchrotron for the optical component and synchrotron self-Compton (SSC) for the γ -rays^{36,37}. The Compton Y parameter, defined as the ratio of the inverse Compton to synchrotron energy losses, is $Y = \nu F_{\nu}(\nu)/\nu F_{\nu}(\nu_{\text{syn}}) \geq 10$, where ν_{syn} is the peak photon energy of the synchrotron νF_{ν} spectrum, to account for the fact that the prompt γ -ray energy is higher than the prompt optical/ultraviolet synchrotron energy. This would imply a third spectral component arising from second-order inverse Compton scattering that peaks at energies around $E_{\text{IC2}} \approx \bar{E}_{\text{IC1}}^2/\bar{E}_{\text{syn}} \approx 23(\bar{E}_{\text{syn}}/20 \text{ eV})^{-1} \text{ GeV}$. Note that the Klein-Nishina suppression becomes important only at $E > 94(\bar{E}_{\text{syn}}/20 \text{ eV})^{-1/2} \Gamma_2 \text{ GeV}$, where $\Gamma = 10^3 \Gamma_2$ is the outflow bulk Lorentz

factor. This third spectral component carries more energy than the observed γ -rays, by a factor $Y \geq 10$, changing the energy budget of this burst and implying that GRB 080319B was even more powerful than inferred from the observed emission. Most of the energy in this burst was emitted in this undetected GeV component, which would have been detected by the *Astro-rivelatore Gamma a Immagini Leggera* (AGILE) satellite had it not been occulted by the Earth, and would have been easily detectable by the recently launched Gamma-ray Large Area Space Telescope (GLAST)³⁸ satellite.

Such bright prompt optical flashes are rare. The exceptional brightness of the optical flash in GRB 080319B implies that the self-absorption frequency ν_a cannot be far above the optical band near the peak time. The optical brightness temperature implies that $300 \leq T/(4/3 \text{ s})^{1/3} \leq 1,400$, and therefore $\Gamma \sim 10^3$, where $t_s = R\Gamma^2 c^{-1}$ is the rough variability timescale in the internal shocks model. Because of the extremely high bulk Lorentz factor Γ , the internal shocks occur at an unusually large radius given by $0.8 \leq R_{\text{sh}}/(4/3 \text{ s})^{1/3} \leq 20$, where $R_{\text{sh}} = R/10^{10} \text{ cm}$, resulting in a relatively low ν_a which in turn allows the optical photons to escape.

Interpretation of the chromatic afterglow

Our broadband data set enabled us to measure the temporal and spectral evolution of GRB 080319B throughout the afterglow. After the prompt phase, the early (minutes to hours) X-ray and optical behaviour are inconsistent with the predictions of the standard afterglow theory, suggesting that they must stem from different emission regions. In particular we find that the optical, X-ray and γ -ray emissions from this burst are explained reasonably well by a two-component jet model^{33,38} (Fig. 4 and Table 2), consisting of an ultra-relativistic narrow jet, surrounded by a broader jet with a lower Lorentz factor. The empirical triple broken power-law function of the X-ray light curve is then interpreted as the superposition of two broken power-law components representing these two jets (Table 2 and Supplementary Fig. 7). This structure, in which the Lorentz factor and energy per solid angle are highest near the axis and decrease outwards, either smoothly or in quasi-steps, qualitatively resembles the results of numerical simulations of jet formation in collapsars³⁹. Further details of the model are given in Supplementary Information; here we summarize the model results and apply them to the observational data.

The optical light curve at $50 \text{ s} < t < 800 \text{ s}$ is dominated by the second optical power-law component, which we interpret as emission from the reverse shock associated with the interaction of the wide jet with the external medium. This segment is consistent with expectations for the high-latitude emission⁴⁰ from a reverse shock ($\alpha = 2 + \beta$) if the cooling frequency ν_c is below the optical band and the injection frequency $\nu_m > 10^{16} \text{ Hz}$. Emission from the reverse shock peaks at $t \sim 50$ s in the optical with a peak flux density of $\sim 2\text{--}3 \text{ Jy}$, but it is initially overwhelmed by the much brighter prompt emission and does not become visible until the latter dies away. The high peak luminosity of the optical reverse shock component soon after the end of the γ -ray emission indicates that the reverse shock was at least mildly relativistic. The GRB outflow could not have been highly magnetized ($\sigma \gg 1$) when it crossed the reverse shock, or the reverse shock would have been suppressed⁴¹, implying that $\sigma \leq 1$, where σ is the ratio of electromagnetic to kinetic energy flux. However, if the outflow was too weakly magnetized ($\sigma \ll 1$), the optical emission would also have been suppressed. Therefore an intermediate magnetization ($0.1 \leq \sigma \leq 1$) is needed to obtain the observed bright emission from the reverse shock^{42,43}.

In contrast, the X-ray light curve in the interval $50 \text{ s} < t < 40 \text{ ks}$ is dominated by the forward shock of the narrow jet component interacting with a surrounding medium produced by the wind⁴⁴ of the progenitor star in the slow cooling case ($\nu_m < \nu_c < \nu_a$, where ν_a indicates the X-ray band). The first break in the X-ray light curve is attributed to a jet break⁴⁵ in this narrow jet (Table 2), leading to a jet half-opening angle of $\sim 0.2^\circ$. Because this break is not seen in the

GRB 090423 reveals an exploding star at the epoch of re-ionization

arXiv:0906.1578v2 [astro-ph.CO] 10 Jun 2009

R. Salvaterra ¹, M. Della Valle ^{2 3 4}, S. Campana ¹, G. Chincarini ^{5 1},
 S. Covino ¹, P. D'Avanzo ^{5 1}, A. Fernández-Soto ⁶, C. Guidorzi ⁷, F. Mannucci
⁸, R. Margutti ^{5 1}, C.C. Thöne ¹, L.A. Antonelli ⁹, S.D. Barthelmy ¹⁰, M. De
 Pasquale ¹¹, V. D'Elia ⁹, F. Fiore ⁹, D. Fugazza ¹, L.K. Hunt ⁸, E. Maiorano
¹², S. Marinoni ^{13 14}, F.E. Marshall ¹⁰, E. Molinari ^{13 1}, J. Nousek ¹⁵, E. Pian ¹⁶
¹⁷, J.L. Racusin ¹⁵, L. Stella ⁹, L. Amati ¹², G. Andreuzzi ¹³, G. Cusumano ¹⁸,
 E.E. Fenimore ¹⁹, P. Ferrero ²⁰, P. Giommi ²¹, D. Guetta ⁹, S.T. Holland ^{10 22}
²³, K. Hurley ²⁴, G.L. Israel ⁹, J. Mao ¹, C.B. Markwardt ^{10 23 25}, N. Masetti ¹²,
 C. Pagani ¹⁵, E. Palazzi ¹², D.M. Palmer ¹⁸, S. Piranomonte ⁹, G. Tagliaferri ¹,
 V. Testa ⁹

¹ INAF, Osservatorio Astronomico di Brera, via E. Bianchi 46, I-23807 Merate (LC), Italy

² INAF, Osservatorio Astronomico di Capodimonte, Salita Miciarelli 16, 80131 Napoli, Italy

³ European Southern Observatory (ESO), 85748 Garching, Germany

⁴ International Centre for Relativistic Astrophysics, Piazzale della Repubblica 2, 45122 Pescara, Italy

⁵ Dipartimento di Fisica G. Occhialini, Università di Milano Bicocca, Piazza della Scienza 3, I-20126 Milano, Italy

⁶ Instituto de Física de Cantabria, CSIC-Univ. Cantabria, Av. de los Castros s/n, E-39006 Santander, Spain

⁷ Dipartimento di Fisica, Università di Ferrara, via Saragat 1, I-44100 Ferrara, Italy

⁸ INAF, Osservatorio Astrofisico di Arcetri, Largo E. Fermi 5, I-50125 Firenze, Italy

⁹ INAF, Osservatorio Astronomico di Roma, Via di Frascati 33, I-00040, Monte Porzio Catone, Rome, Italy

¹⁰ NASA, Goddard Space Flight Center, Greenbelt, MD 20771, USA

¹¹ Mullard Space Science Laboratory (UCL), Holmbury Rd, Holmbury St. Mary, Uxbridge, RH5 6NT, UK

¹² INAF, IASF di Bologna, via Gobetti 101, I-40129 Bologna, Italy

¹³ INAF, Fundación Galileo Galilei, Rambla José Ana Fernández Pérez, 7 38712 Breña Baja, TF - Spain

¹⁴ Università degli Studi di Bologna, via Ramanzini, 1, Bologna, Italy

¹⁵ Department of Astronomy and Astrophysics, Pennsylvania State University, University Park, PA 16802, USA

¹⁶ INAF, Trieste Astronomical Observatory, Via G.B. Tiepolo 11, I-34143 Trieste, Italy

¹⁷ Scuola Normale Superiore, Piazza dei Cavalieri 1, 58100 Pisa, Italy

¹⁸ INAF, Istituto di Astrofisica Spaziale e Fisica Cosmica di Palermo, Via Ugo La Malfa 153, 90146 Palermo, Italy

¹⁹ Los Alamos National Laboratory, P.O. Box 1683, Los Alamos, NM, 87545, USA

²⁰ Thüringer Landessternwarte Tautenburg, Sternwarte 5, D-97778, Tautenburg, Germany

²¹ ASI Science Data Center, ASDC c/o ESRIN, via G. Galilei, 00044 Frascati, Italy

²² Universities Space Research Association, 10211 Winopin Circle, Suite 500, Columbia, MD, 21044, USA

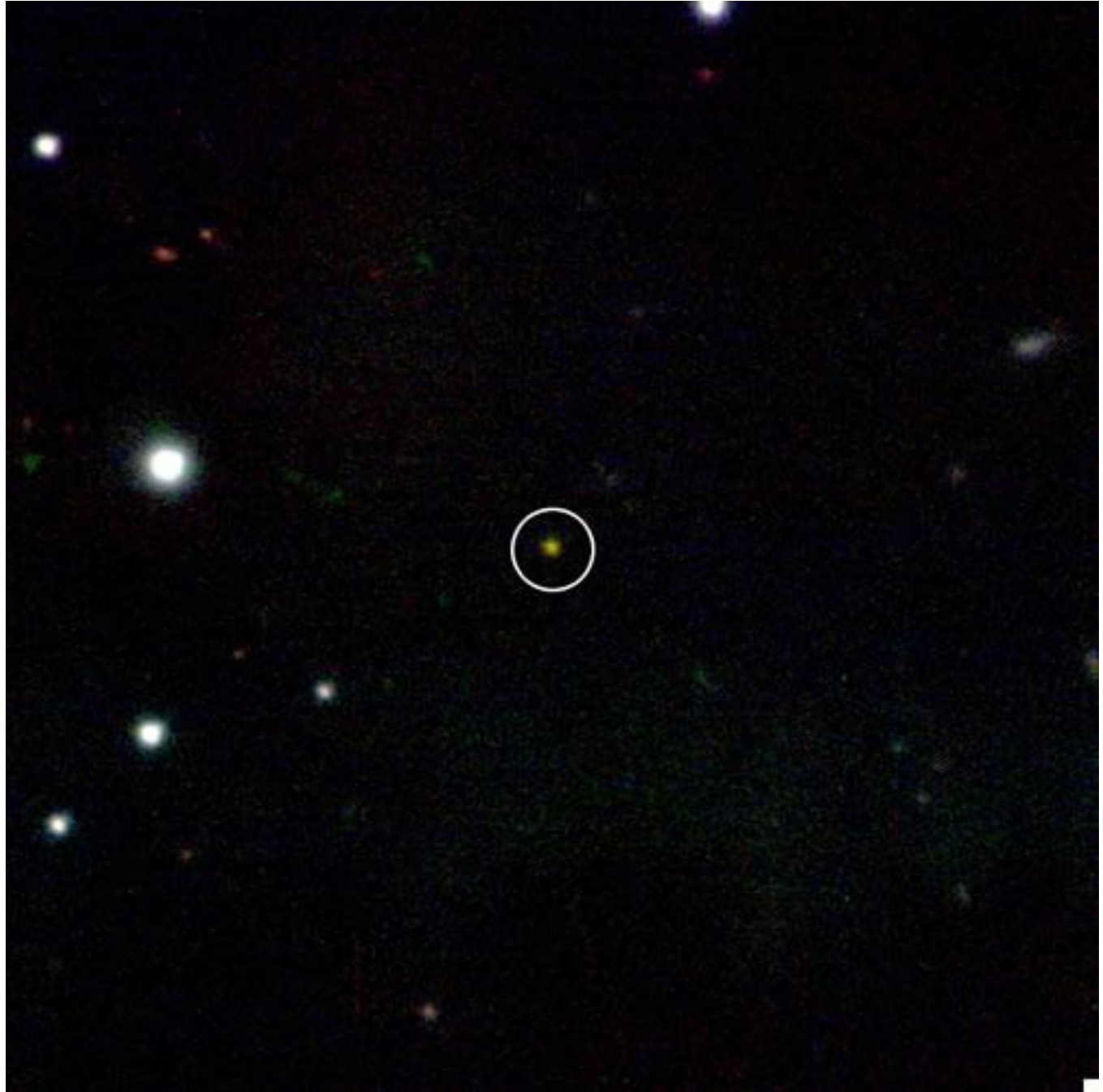
²³ Centre for Research and Exploration in Space Science and Technology, Code 688.8, Greenbelt, MD, 20771, USA

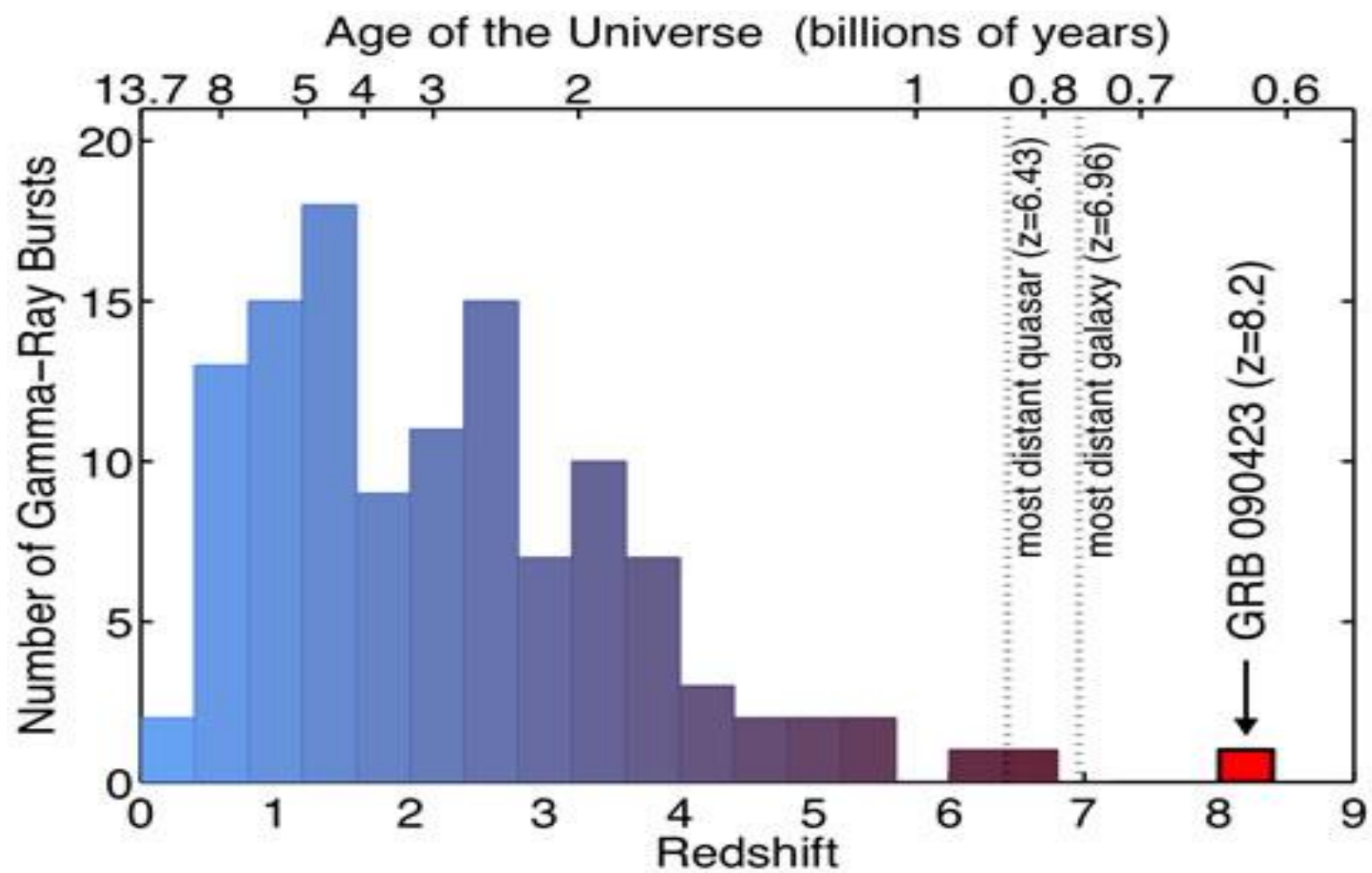
²⁴ Space Sciences Laboratory, 7 Gauss Way, University of California, Berkeley, CA 94720-7450, USA

²⁵ Department of Astronomy, University of Maryland, College Park, MD 20742, USA

The observation of the very early stages of the Universe represents one of the main challenges of modern cosmology. 200-300 million years after the Big Bang stars began to form, thus providing the Universe with the first sources of light and heat after the Big Bang.

GRB090423





Credit: Edo Berger (Harvard/CfA)

Low Frequency ARray



The ambitious successor of the early radio work of Giorgio using the new technology

Organisation: ASTRON

Location: 3km north of Exloo, the Netherlands (core)

Wavelength: 30 to 1.3 m (radio)

Built: 2006 – 2009

Telescope style: phased array of ~10,000 dipole antennas

Diameter: 1000 km or more

Collecting Area: up to 1 km²

Abstract

When gamma-rays emerge from a central source they may undergo Compton scattering in surrounding matter. The resulting Compton-scattered electrons radiate. Coherent radiation by such Compton electrons follows nuclear explosions above the Earth's atmosphere. Particle acceleration in instabilities produced by Compton electron currents may explain the radio emission of SN1998bw. Bounds on coherent radiation are suggested for supernovae and gamma-ray bursts; these bounds are very high, but it is unknown if coherent radiation occurs in these objects.

High altitude (exospheric) nuclear explosions are well known to produce striking electromagnetic phenomena on the surface of the Earth. These phenomena, termed HEMP (High altitude ElectroMagnetic Pulse) or EMP (Karzas and Latter 1962, 1965) occur when prompt gamma-rays following nuclear fission, radiative neutron capture or inelastic neutron scattering suffer Compton scattering in the upper atmosphere. The Compton electrons, with energies typically ~ 1 MeV, are preferentially directed along the direction of the incident gamma-rays, radially away from the gamma-ray source, and move at a speed close to the speed of light. They are deflected by the geomagnetic field and radiate synchrotron radiation. Because the gamma-rays and Compton electrons are produced over an interval $< 10^{-7}$ sec, shorter than the characteristic gyroperiod of the radiation ($\sim 10^{-8}$ sec, allowing for the relativistic energy of the electrons) this radiation is coherent; it may be regarded as the effect of a continuously distributed time-dependent current density, rather than as the radiation of individual electrons. The number of radiating electrons is very large so that the currents and coherent radiation intensity are high, and are limited by the condition that the radiation field not exceed the geomagnetic field, for the radiation field of the Compton current acts to screen the geomagnetic field. In fact, the radiation may be crudely approximated as the diamagnetic field exclusion by the conducting swarm of Compton electrons. In atmospheric EMP the Compton electrons produce large numbers of low energy electrons by collisional ionization, and the effects of these electrons on the emergent radiation are the chief subject of the published calculations.

Analogous phenomena may be produced by astronomical events. Karzas and Latter (1965) indicate a threshold gamma-ray fluence for the observation of EMP of $\sim 10^{-8}$ erg/cm². This is less than the fluence of many observed gamma-ray bursts (GRB), in some cases by more than two orders of magnitude. However, GRB do not produce observable EMP in the Earth's atmosphere because their emission occurs over a duration from milliseconds to minutes, several orders of magnitude (even for the shortest GRB) longer than the electrons' gyroperiod in the geomagnetic field. As a result the EMP, although coherent in the sense that many electrons radiate in phase, is much reduced in amplitude because it is an incoherent average over a very large number of cycles of electron gyromotion; the

1981

Palumbo¹ G.G.C., Maccacaro^{2,3} F., Panagia² N., Vettolani² G.,
Zamorani² G.

¹ ISTITUTO F.E.S.R.E. - CNR -, Bologna, Italy

² ISTITUTO DI RADIOASTRONOMIA - CNR - Bologna, Italy

³ Center for Astrophysics, Cambridge, USA.

ABSTRACT:

During a search for X-ray emission from Supernova 1979c, the parent galaxy M100 (NGC 4321) was repeatedly observed with the IPC and HRI instruments aboard the Einstein X-ray Observatory. The X-ray data reveal two possible sources in the arms of the spiral galaxy, two components in the nuclear bulge and extended X-ray emission from the central part of the galaxy (160x160 square arc seconds centered on the nucleus). We find that the extended X-ray emission cannot be explained in terms of inverse Compton effect on radio, optical or 3 K blackbody photons but rather it is likely to originate from supernova remnants (M100 is indeed a prolific supernova producer) and/or early type stars. As for M100 as a whole, the ratio of X-ray to optical luminosity places it half way between "normal galaxies" e.g. M31 or M33 and peculiar or active galaxies.

During an unsuccessful search for X-ray emission from Supernova 1979c in M100 (NGC 4321) (Palumbo et al. 1981), a wide field containing the galaxy and the surrounding region was observed with the Imaging Proportional Counter (IPC) and the High Resolution Imager (HRI) aboard the Einstein Observatory. The instrumentation has been described in detail by Giacconi et al. (1979). Data concerning SN 1979c have been presented elsewhere (Palumbo et al. 1981). From the first HRI observation, the galaxy appeared quite interesting because of evidence of multiple structures in the nucleus and rather high integrated nuclear emission (1.5×10^{40} erg s⁻¹) in the 0.1 - 4.5 keV band. Subsequent observations both at ultraviolet (IUE; Panagia et al. 1980a) and optical wavelengths showed the presence of condensations with characteristics of low excitation HII regions. These appeared to be at the roots of the spiral arms. Furthermore, a 21 cm VLA map (Weiler et al. 1981) also shows a complex structure in the nucleus of M100 as well as evidence of extended emis-

**Start of Giorgio's
Group in Bologna
In X-ray Astronomy**

-
- Member of Astronomy Working Group
 - Member of Space Station User Panel
 - Mission Scientist for INTEGRAL
-

Giorgio, Best Wishes for the Future
